Published in final form as:

Loveday, S. M., Rao, M. A., Creamer, L., & Singh, H. (2010). Rheological Behavior of High-Concentration Sodium Caseinate Dispersions. Journal of Food Science, 75(2), N30-N35.

doi: 10.1111/j.1750-3841.2009.01493.x

Rheological Behavior of High-concentration Sodium Caseinate Dispersions

SIMON M. LOVEDAY[1], M. ANANDHA RAO[1,2], LAWRENCE K. CREAMER[1], AND HARJINDER SINGH[1]

[1] Riddet Institute, Massey University, Private Bag 11 222, Palmerston North 4474, New Zealand

[2]Author Rao is also with Food Science and Technology Dept., Cornell Univ., Geneva, NY 14456, U.S.A. Direct inquiries to author Rao (E-mail: mar2@cornell.edu.), Tel. 315-521-9252.

Short title: Rheology of Concentrated Sodium Caseinate…

Journal section: Nanoscale Food Science, Engineering and Technology

Abstract

Apparent viscosity and frequency sweep (*G'*, *G"*) data for sodium caseinate dispersions with concentrations of approximately 18–40% w/w were obtained at 20°C; colloidal glass behavior was exhibited by dispersions with concentration ≥ 23% w/w. The *G'–G"* crossover seen in temperature scans between 60 and 5°C was thought to indicate gelation (low-temperature crossover). Temperature scans from 5 to 90°C revealed gradual decrease in G', followed by plateau values. The gelation and end of softening temperatures of the dispersions increased with the concentration of sodium caseinate. From an Eldridge–Ferry plot, the enthalpy of softening was estimated to be 29.6 kJ mol^{-1}.

Keywords: sodium caseinate, viscosity, modulus, colloidal glass, gelation, softening

Introduction

The size range of colloidal (Brownian) particles is generally considered to be from about 1 nm to 1 μm (Russel and others 1989). In colloidal dispersions, Brownian motion promotes collisions between pairs of colloidal particles and interparticle forces determine whether or not two colliding particles aggregate. Very high viscosities and glassy states are found in high-concentration dispersions of colloidal hard spheres, sodium caseinate, and the globular proteins: bovine serum albumin and β-lactoglobulin (Loveday and others 2007).

Caseins make up about 80% of the protein in milk; they are used as emulsifiers, foaming agents, and thickening agents. The structures of caseins are not amenable to examination by X-ray crystallography or high-field nuclear magnetic resonance because they cannot be crystallized or have stable time-invariant three-dimensional structures at low pH. The two major caseins are α_{s1}-casein and β-casein (approximately 35% each of the whole casein mixture). These two proteins behave slightly differently from one another and very differently from the well-known globular proteins, such as serum albumin, lysozyme, and the fibrous proteins that make up muscles, skin, etc.

In milk, the casein is aggregated with calcium phosphate as casein micelles (mean size about 300 nm). After the calcium phosphate is removed, the resulting sodium caseinate exists in solution mainly as a mixture of casein monomers and casein nanometer-scale particles (10–20 nm); further, gels may be produced from dispersions of sodium caseinate by heating, acidification, and high-pressure processing (Dickinson 2006). In a mixed casein system such as sodium caseinate, different caseins interact with each other to form associated structures, which exist as a dynamic system of casein monomers, casein complexes, and aggregates (Lucey and others 2000). The average radius of gyration of caseinate aggregates has been shown to be in the range 22–48 nm, depending on the method of preparation; the aggregates have been shown to be not spherical but highly elongated structures. The extent of aggregation of sodium caseinate depends on the relative proportions of the different monomeric caseins and also on the temperature, pH, ionic strength, and calcium ion concentration (Dickinson 2006).

Models for estimating the viscosity of concentrated dispersions of solids are based on the volume fraction (ϕ) of the suspended solids and the relative viscosity of the dispersion, $\eta_r = (\eta/\eta_s)$, where η is the viscosity of the dispersion and η_s is the viscosity of the continuous phase (Metzner 1985). At high concentrations of solids of uniform size, one widely used equation is that of Krieger and Dougherty (1959), which is based on the assumption that equilibrium exists between individual spherical particles and dumbbells that continuously form and dissociate:

$$\eta_r = \left(1 - \frac{\phi}{\phi_{max}}\right)^{-[\eta]\phi_{max}} \qquad (1)$$

Where $[\eta]$ and ϕ_{max} are the intrinsic viscosity and the maximum packing fraction of solids, respectively. Theoretically, $[\eta]$ should be 2.5 for rigid spheres and ϕ_{max} should be about 0.62–0.65 for spheres of uniform diameter (Krieger 1985). For polydisperse spherical particles in Newtonian fluids, ϕ_{max} is higher because small particles may occupy the space between the larger particles. During flow, they act as a lubricant for the flow of the larger particles, thereby reducing the overall viscosity (Servais and others 2002); for a given particle concentration (ϕ), the viscosity decreases with increasing polydispersity (particle size distribution width).

Small-amplitude oscillatory tests can be used to study the viscoelastic properties of dispersions. The dependence of the storage modulus, *G'*, and the loss modulus, *G"*, on the oscillatory frequency (ω) in the linear viscoelastic region is one set of useful information. If *G"* > *G'*, the material is behaving predominantly as a viscous liquid. However, if *G'* > *G"*, the material is behaving predominantly as a solid. Mason and Weitz (1995) reported that, as the volume fraction of colloidal silica hard spheres (radius a = 0.21 μm) approached that of the glass transition, *G'* became larger than *G"*. Thus, the dynamic rheological data for the dispersions were strongly modified to solid-like behavior as ϕ approached ϕ_G.

Gelation and softening/melting temperatures are often determined from the crossing of *G'* and *G"* during temperature sweep experiments; however, the so-defined transition temperatures or gelation times depend on the chosen frequency (Rao 2007). Using temperature sweep data at 0.1 Hz, heating-induced gelation and thermo-reversibility of the gels were demonstrated for sodium-caseinate-based oil-in-water emulsions containing a controlled amount of added ionic calcium (15–30 mM) (Dickinson and Casanova 1999). Carr and Munro (2004) studied the phenomenon of gelation by the cooling of 14% w/w sodium caseinate solutions at different ionic strengths; they determined the gel–sol transition temperatures at 1 Hz. This phenomenon may be attributed to the increased relative contribution of attractive interchain interactions (especially hydrogen bonding) at lower temperatures (Dickinson and Casanova 1999).

In a mixed casein system, such as sodium caseinate variable degrees of de-mixing at the sub-micellar level and improvement in co-mixing with concentration can be expected (Farrer and Lips 1999). An important property of the hydrophobic effect is entropy driven de-mixing. Guo and others (1996) reported that the relative hydrophobicity and the viscosity of a 6% sodium caseinate dispersion decreased on heating at 132°C due to the changes in structure of the protein. Therefore, the hydrophobic effect plays an important role in the rheological behavior of sodium caseinate dispersions when the concentration and temperature are changed.

Zhou and Mulvaney (1998) reported complex modulus, *G**, vs. temperature (5-70°C) profiles, during heating rennet casein-water-milk fat dispersions; their concentrations were reported as ratios (e.g., casein to water). Farrer and Lips (1999) measured the osmotic pressure, p, of sodium caseinate dispersions as a function of concentration (C) and temperature. Their data showed a temperature-independent scaling $p \sim C^{3.25}$ for C > 10% w/v. They suggested a demarcation into two separate regimes: below close packing and above close packing. The first regime is expected to be sensitive to attractive interactions between sub-micelles and the second is expected to be dominated by repulsive forces of micellar crowding/interpenetration. They obtained zero-shear viscosity data on dispersions of sodium caseinate (pH 6.8, 0.1 M NaCl) over a range of concentrations from about 3 to 28% w/v. It was suggested that the experimental concentration versus relative viscosity data can be attributed to caseinate particle aggregation below close packing and to a rheological and 'soft particle' response of the sub-micelles above close packing. At high C, the scaling was apparently $\eta_r \sim C^{12}$ and the concentrated sodium caseinate dispersions showed the viscoelastic behavior of entanglement polymer systems.

From light scattering measurements on dilute solutions, up to about 5%, HadjSadok and others (2008) noted that sodium caseinate associates into small well-defined aggregates with an aggregation number that depended on the temperature, pH, and ionic strength. Small-angle X-ray scattering data on sodium caseinate dispersions with NaCl concentrations between 0 and 250 mM showed that, at a relatively low concentration (C = 10 g.L^{-1}), the effect of interaction between the caseinate particles was weak, whereas, at a high concentration (C = 120 g.L^{-1}), the particles were close packed; the distance between the

caseinate particles was found to be about 20 nm, consistent with a solution of close-packed caseinate particles (Pitkowski and others 2008). They suggested that perhaps star-shaped aggregates were formed with a hydrophobic centre and a hydrophilic (charged) corona. The same authors interpreted the effect of the temperature on the concentration dependence of the zero-shear viscosity, η_0, in terms of an effective volume fraction of the caseinate aggregates that increased with decreasing temperature. The relaxation process was characterized by a broad distribution of relaxation times and slowed down rapidly with increasing effective volume fraction, i.e., increasing concentration or decreasing temperature. It was also noted that the sodium caseinate particles are soft, partially draining, charged, and have polydisperse size distribution (Pitkowski and others 2008).

The objectives of this study were to examine the rheological behavior of colloidal glass dispersions of sodium caseinate: (1) to obtain apparent viscosity versus concentration data and to test the applicability of the Krieger–Dougherty model, (2) to examine *G'* and *G"* from frequency sweep data to determine the concentration at which solid-like behavior is first seen as well as the behavior at higher concentrations, and (3) to determine the gelation and softening temperatures from the *G'*–*G"* during the cooling and heating of the dispersions, respectively. It should be noted that dispersions of high concentrations, previously not examined, were studied in this work.

Materials and Methods

The procedure used in this work to prepare sodium caseinate dispersions in the concentration range 18–40% w/w was adapted from the method developed by Davies and others (1969) to adjust the moisture content of flour. The buffer, 25mM phosphate, pH 6.8, and 70mM NaCl, was added drop wise to boiling liquid nitrogen in a ceramic mortar and, once frozen, was ground to a fine powder with a ceramic pestle. Frozen powdered buffer was weighed into a precooled metal container and the required mass of sodium caseinate powder was added, followed by sufficient liquid nitrogen to suspend and mix the two powders. When the liquid nitrogen had boiled off, the mixture was transferred to 1.5 mL plastic tubes and allowed to thaw and hydrate at 4°C overnight. Immediately prior to rheological measurements, the sodium caseinate dispersions were heated to 60°C in a water bath and then centrifuged for 10 min at 14,000 *g* to remove air. The actual concentration of sodium caseinate in each sample was determined after heating the sample at 108°C for 1–2 days.

Steady shear and dynamic rheological data were obtained at 20°C with a Paar Physica MRC301 rheometer using cone and plate geometries; a 40 mm diameter cone was used at lower concentrations and a 10 mm diameter cone was used at higher concentrations. It took a long time to get data at very low shear rates with the rheometer. Therefore, to avoid dehydration of samples, lower shear rates used were not below $0.5s^{-1}$ or $0.2s^{-1}$ in some cases. With the high concentration dispersions, often, at shear rates greater than about 10 s^{-1}, the Weissenberg ("rod climbing") effect was encountered resulting in the flow of the sample out of the cone-plate geometry. However, there were few problems obtaining frequency sweep data that were important in order to examine solid-like behavior and colloidal glass transition of the dispersions. Zero-shear viscosities were obtained by fitting the Cross model to the apparent viscosity–shear rate data (Figure 1). It is noted that the values given by the Cross model have been found to be reliable for several food polymer dispersions (Rao 2007, Chapter 4).

In separate experiments, cooling, 60–5°C, and heating, 5–90°C, triplicate scans were performed at 3% strain, using the 10 mm diameter cone–plate geometry; a fixed rate of cooling and heating, 2.5°C.min^{-1}, was used. The values of *G'*, *G"*, and temperature that were recorded were used to estimate the gelation and softening temperatures. To ascertain if wall slip affected the magnitudes of *G'* and *G"*, data were obtained with a serrated plate system; however, the modulus-temperature profiles were similar to those obtained using the standard measuring systems.

Results and Discussion

Zero-shear viscosities

The modified Cross model (Equation 2), in which the infinite shear viscosity, η_∞, was neglected, was used to fit the apparent viscosity versus shear rate data and to obtain values of the zero-shear viscosity:

$$\eta_a = \frac{\eta_0}{1+(\alpha_c \dot{\gamma})^m} \qquad (2)$$

Where, α_c is a time constant related to the relaxation time of the polymer in solution and *m* is a dimensionless exponent. Because the magnitude of η_∞ of a food polymer dispersion with a concentration of practical interest is usually very low, η_∞ can often be neglected (Rao 2007).

In Figure 1, apparent viscosity versus shear rate data for several sodium caseinate dispersions and the Cross model fits to the data are shown. It can be seen that the sodium caseinate concentration had a marked effect on the apparent viscosity; at the higher concentrations, at shear rates higher than the zero-shear viscosity range, the dispersions exhibited marked shear-thinning behavior. The Cross model fitted the data well and, as noted later, values of the relative viscosity followed the trend of the data of Farrer and Lips (1999). Nevertheless, it is recognized that limiting viscosity data at low shear rates were not available at high concentrations. The estimated values of the zero-shear viscosities and, in parentheses, their standard errors were: 15%, 1.28 Pa s (0.02); 20.0%, 73.0 Pa s (0.54); 25.0%, 7.29 kPa s (137); 29.0%, 25.9 kPa s (843), and 31.6%, 39.2 kPa s (1692).

Farrer and Lips (1999) obtained zero-shear viscosity data for dispersions of sodium caseinate (pH 6.8, 0.1 M NaCl) over a range of concentrations from about 3 to 28% w/v. The corresponding values of relative viscosity were calculated using solvent viscosity = 1 mPa s. Panouille and others (2005) obtained zero-shear viscosity data for dispersions of phosphocaseinate (pH 6.0, polyphosphate 2% w/v); the phosphocaseinate was obtained after the colloidal calcium phosphate had been removed from the casein micelles. The relative viscosities of the phosphocaseinate dispersions were higher than those of the sodium caseinate dispersions (Farrer and Lips 1999). An empirical model, based on concentration, *C*, (instead of volume fraction) was used to fit the viscosity data of the phosphocaseinate dispersions up to a concentration of approximately 10% w/v:

$$\eta_r = \left(1 - \frac{C}{C_c}\right)^{-2} \qquad (3)$$

Our viscosity data are shown along with those of Farrer and Lips (1999) and those based on Panouille and others (2005) in Figure 2. It can be seen that the relative viscosity increases gradually with concentration up to about 10% and then steeply at higher concentrations (Figure 2). Pitkowski and others (2008) noted that this behavior was also found in multi-arm star polymers and polymeric micelles. Our high-end sodium caseinate dispersions were of higher concentration than in previous studies (Farrer and Lips 1999; Panouille and others 2005) and our viscosity data were in good agreement with the extrapolated data of Farrer and Lips (1999). The dashed line in Figure 2 represents relative viscosity values of the phosphocaseinate dispersions predicted by the empirical model (Equation 3).

Also shown in Figure 2 (solid line) are values of relative viscosity predicted by the Krieger–Dougherty model with $[\eta]$ = 2.5 and ϕ_{max} = 0.65. It is interesting to note that the values predicted by the model were lower than the data up to a concentration of about 14% w/w, but increased more steeply than the data at higher concentrations. Because of uncertainties in the determination of the sodium caseinate particle volume fraction, the polydispersity of the particles, and their softness, the Krieger–Dougherty rheological model developed for hard-sphere dispersions predicted the trends accurately but not the absolute values of viscosity.

Frequency sweep rheological data

In Figure 3, we show our frequency sweep data obtained in the linear viscoelastic range. We note that the concentrated Na-caseinate dispersions showed the viscoelastic behavior of entanglement polymer systems, as opposed to gel systems, previously noted by Farrer and Lips (1999). With an increase in the sodium caseinate concentration, the trend in the frequency sweep data was for values of *G'* to be greater than those of *G"* over an increasing range of shear: at 23% w/w, values of *G'* were greater than those of *G"* for $\omega > 2$ rad s^{-1}; at 31.6% w/w, *G'* > *G''* for $\omega > 0.3$ rad s^{-1}; at 40.1% w/w, *G'* > *G''* over the entire range of frequency. Thus, sodium caseinate dispersions with concentrations≥ 23% w/w exhibited colloidal glass behavior; as the concentration of sodium caseinate was increased, the dispersions exhibited increasing solid-like behavior and the dispersions with concentrations greater than 40.1% w/w exhibited solid-like rheological behavior over the entire range of oscillatory frequencies.

Cooling and heating scans, and gelation and melting temperatures

Cooling and heating scans were performed at 1.0 Hz on sodium caseinate dispersions with concentrations between 18.1 and 41.9% w/w; the cooling scans between 60 and 5°C were conducted first, followed by the heating scans between 5 and 90°C. The magnitudes of *G'* and *G"* during the cooling and heating scans were plotted and the gelation, point A, and softening, point B, temperatures, were determined. For clarity of illustration, only every fifth point recorded for a 33.8% w/w sodium caseinate dispersion is shown in Figure 4. The average gelation temperatures of the sodium caseinate dispersions and their standard deviations, from three replicates at each concentration, are shown in Figure 5. The increase in gelation temperature with concentration was found to be linear (Figure 5). The gel formation on cooling may be attributed to the increased relative contribution of attractive interchain interactions (especially hydrogen bonding) at lower temperatures (Dickinson and Casanova 1999).

In the heating scans, values of G' of each dispersion decreased continuously with increase in temperature followed by a transition to a plateau region (Figure 4). The two likely phenomena noted earlier, decrease in effective volume fraction (Pitkowski and others 2008)

and hydrophobicity of sodium caseinate (Guo and others 1996), may be ascribed to the continuous decrease in *G'* of the dispersions with increase in temperature. The *G** vs. temperature profiles of Zhou and Mulvaney (1998) during heating casein-water-milk fat dispersions were similar to that in Figure 4; they referred to three zones as: rubbery solid, transition, and melt regions. The decrease in *G** was attributed to loss of physical cross links in the caseinate matrix. However, with values of *G'* being lower than those of *G''* once the temperature was higher than the gel temperature (Figure 4), it would not be appropriate to characterize a *G'-G''* cross-over as melting phenomenon. Aggregation of sodium caseinate and precipitation were reported on heating dilute solutions of sodium caseinate (HadjSadok and others 2008). However, Pitkowski and others (2008), from the same laboratory, did not report precipitation in a 20% sodium caseinate dispersion heated to 90°C. Our *G'*-temperature profiles reflect a viscoelastic material whose elasticity (magnitude of *G'*) decreased continuously as the temperature was increased, probably due to the loss of physical cross links in the caseinate matrix until attaining plateau values.

The plateaus in the values of *G'* also seem to be likely due to the dispersions reaching either a nearly constant value of volume fraction of sodium caseinate aggregates or hydrophobicity. Based on a number of data points in the plateau region, n, the average plateau values of *G'* and their standard deviations, SD, were calculated: 31.3 Pa (n=32, SD=1.23), 31.3 Pa (n=25, SD=1.56), 32.4 Pa (n=13, SD=1.61), and 41.4 Pa (n=13, SD=3.6) for the sodium caseinate dispersions with concentrations 18.1, 22.0, 33.8, and 41.9% w/w, respectively.

Considering that the decrease in *G'* reflected softening phenomenon, the temperatures at which the continuous decrease in *G'* ended and the transition to the plateau region began were designated as softening temperatures (T_{soft}); further, their magnitudes were estimated from the intersection (not shown here) of the linear regions of the continuously decreasing and the plateau segments on plots of log *G'* vs. temperature plots. The average values of T_{soft}, also shown in Figure 5, increased with increase in the concentration of sodium caseinate, likely due to improvement of co-mixing with concentration (Farrer and Lips 1999).

Values of *G''* were nearly the same in magnitudes as those recorded during the cooling scans (for example, see Figure 4). It is noted that values of *G''*, which reflect viscous dissipation, should be relatively unaffected by the volume fraction of sodium caseinate aggregates. The continuous decrease in the values of *G''* with increase in temperature was likely due to decrease in hydrophobicity of sodium caseinate (Guo and others 1996). Unlike values of *G'*, those of *G''* did not exhibit plateau values likely due to the negligible influence of the volume fraction of sodium caseinate aggregates.

Barreto and others (2003) reported that the effect of temperature, over the range 17°C to 30°C, on the Newtonian viscosity (η) of sodium caseinate dispersions with concentrations 10.5 to 13.0% (w/w) followed the Arrhenius equation:

$$\infty \exp (E_a/RT) \qquad (4)$$

Where, η is the viscosity, η_∞ is the infinite-temperature viscosity, E_a, is the activation energy of flow, R is the gas constant, and T is the absolute temperature. However, as illustrated for the complex viscosity data obtained during cooling and heating scans on the 18.1 and 41.9% w/w dispersions (Figure 6), the Arrhenius relationship was not applicable for data over a wide range of temperatures. It should be noted that the limited applicability of the Arrhenius equation has also been reported for several foods (Chapter 3, Rao 2007). Pitkowski and

others (2008) also reported a similar observation for a 20% sodium caseinate dispersion over the range 5-90°C. They suggested that the decrease in viscosity with temperature was due to a decrease in the effective volume fraction, less than 40% between 10 and 90°C, of sodium caseinate aggregates with increase in temperature; the decrease in the effective volume fraction with increasing temperature was caused by a reduction in the repulsive interaction between the aggregates. We note that the decrease in viscosity with temperature may have been also due to a concomitant decrease in hydrophobicity of the dispersions.

Eldridge and Ferry (1954) studied the relationship between the melting temperature (T_m) and the concentration (*C*) and molecular weight (*M*) of gelatin gels. They found linear relationships between ln (*C*) and $1/T_m$, and between ln (*M*) and T_m . Assuming an equilibrium binary association of polymer chains and using the van't Hoff law, they suggested the following relationship from which it is possible to calculate the enthalpy (ΔH_m) of the crosslinks and to get some information about the stability of the junction zones.

$$-\left[\frac{d\ln C}{dT_m}\right]_{MW} = \frac{\Delta H_m}{RT^2} \qquad (4)$$

This approach was satisfactorily applied to other biopolymer gelled systems, including agarose, high-methoxyl pectin/dimethyl sulfoxide gels, κ-carrageenan, and low-methoxyl pectin/ Ca^{2+} and low-methoxyl pectin/ Ca^{2+}/sucrose systems (p. 373, Rao 2007).

While the rheological data on the sodium caseinate dispersions did not exhibit *G'-G''* crossover melting temperatures, they underwent softening, so that the enthalpy of their cross links can be determined from an Eldridge- Ferry plot based on the softening temperature. Figure 7 is a plot of ln (sodium caseinate concentration, %) vs. $1/T_{soft}$ of the sodium caseinate dispersions. From the slope of the straight line, the enthalpy of melting was determined to be 29.6 kJ.mol^{-1}. We note that this value is much lower than that of gelatin gels, 205–305 kJ.mol^{-1} (Rao 2007, p. 373), but higher than the values reported for gels of whey protein isolate, dialyzed against EDTA, pH 8.0, 10.25–10.75%, aged for 17 and 65 h: 2.94 and 3.59 kJ.mol^{-1}, respectively (Rector and others 1989). It is also noted that Rector and others (1989) used displacement of a metal sphere to detect melting temperatures.

Conclusions

Sodium caseinate dispersions with concentrations of approximately 23–40% w/w exhibited high values of viscosity and solid-like behavior, characteristic of the colloidal glassy state. The apparent viscosities of the dispersions were in line with those of Farrer and Lips (1999). Because of uncertainty in the determination of the sodium caseinate particle volume fraction, the polydispersity and non-spherical shape of the particles, and their softness, the Krieger–Dougherty rheological model developed for hard-sphere dispersions did not predict accurately the absolute values of viscosity. Gelation and softening temperatures were estimated from *G'* and *G"* data obtained from cooling and heating scans; the temperatures increased linearly with the concentration of sodium caseinate. From an Eldridge–Ferry plot of the softening temperature data, the enthalpy of softening was estimated to be 29.6 kJ.mol^{-1}.

Acknowledgments

We thank Sina Hosseiniparvar for his skilful assistance with rheological measurements, and Fonterra Co-operative Group Ltd and the New Zealand Foundation for Research, Science and Technology for funding this work.

References

Barreto, PLM, Roeder, J, Crespoa JS, Maciel GR, Terenzi H, Piresa ATN, Soldi V. 2003. Effect of concentration, temperature and plasticizer content on rheological properties of sodium caseinate and sodium caseinate/sorbitol solutions and glass transition of their films. Food Chem 82: 425–31.

Carr AJ, Munro, PA. 2004. Reversible cold gelation of sodium caseinate solutions with added salt. J Dairy Res 71:126–8.

Davies RJ, Daniels NWR, Greenshields RN. 1969. An improved method of adjusting flour moisture in studies on lipid binding. J Food Technol 4(2):117–23.

Dickinson E. 2006. Structure formation in casein-based gels, foams, and emulsions. Colloids Surf A 288:3–11.

Dickinson E, Casanova H. 1999. A thermoreversible emulsion gel based on sodium caseinate. Food Hydrocoll 13(4):285–9.

Eldridge JE, Ferry JD. 1954. Studies of the cross-linking process in gelatin gels. III. Dependence of melting point on concentration and molecular weight. J Phys Chem 58:992–5.

Farrer D, Lips A. 1999. On the self-assembly of sodium caseinate. Int Dairy J 9:281–6.

Guo MR, Fox PF, Flynn A, Kindstedt PS. 1996. Heat induced modifications of the functional properties of sodium caseinate. International Dairy Journal, 6, 473–483.

HadjSadok A, Pitkowski A, Taco N, Benyahia L, Moulai-Mostefa N. 2008. Characterisation of sodium caseinate as a function of ionic strength, pH and temperature using static and dynamic light scattering. Food Hydrocolloids 22:1460–66.

Krieger IM. 1985. Rheology of polymer colloids. In: Buscall R, Corner T, Stageman JF, editors. Polymer colloids. New York: Elsevier Applied Science. p. 219–46.

Krieger IM, Dougherty TJ. 1959. A mechanism for non-Newtonian flow in suspensions of rigid spheres. Trans Soc Rheol 3:137–52.

Loveday SM, Creamer LK, Singh H, Rao MA. 2007. Phase and rheological behavior of high-concentration colloidal hard-sphere and protein dispersions. J Food Sci 72(7):R101–7.

Lucey JA, Srinivasan M, Singh H, Munro PA. 2000. Characterisation of commercial and experimental sodium caseinates by multi-angle laser light scattering and size-exclusion chromatography. J Agric Food Chem 48:1610–6.

Mason TG, Weitz, DA. 1995. Linear viscoelasticity of colloidal hard sphere suspensions near the glass transition. Phys Rev Lett 75:2770–3.

Metzner AB. 1985. Rheology of suspensions in polymeric liquids. J Rheol 29:739–75.

Panouille M, Benyahia L, Durand D, Nicolai T. 2005. Dynamic mechanical properties of suspensions of micellar casein particles. J Colloid Interface Sci 287:468–75.

Pitkowski A, Durand D, Taco N. 2008. Structure and dynamical properties of suspensions of sodium caseinate. J Colloid Interface Sci 326:96–102.

Rao, MA. 2007. Rheology of fluid and semisolid foods: principles and applications. 2nd ed. New York: Springer. 480 p.

Rector DJ, Kella NK, Kinsella JE. 1989. Reversible gelation of whey proteins: melting, thermodynamics and viscoelastic behavior. J Texture Stud 20:457–71.

Russel WB, Saville DA, Schowalter WR. 1989. Colloidal dispersions. Batchelor GK, series editor. Cambridge, UK: Cambridge University Press. 525 p.

Servais C, Jones R, Roberts I. 2002. The influence of particle size distribution on the processing of food. J Food Eng 51:201–8.

Zhou N, Mulvaney SJ. 1998. The effect of milk fat, the ratio of casein to water, and temperature on the viscoelastic properties of rennet casein gels. J Dairy Sci, 81:2561–71.

Nomenclature

a	particle radius, m
C	concentration, kg.m^{-3}
G'	elastic or storage modulus, Pa
G''	loss modulus, Pa
G^*	complex modulus,
m	dimensionless exponent, -
p	osmotic pressure, Pa
R	gas constant, J mol^{-1} K^{-1}
T	temperature, °C, K
T_m	melting temperature, °C, K
T_{soft}	softening temperature, °C, K
α_c	time constant, s
ΔH_m	enthalpy of melting, kJ mol^{-1}
$\dot{\gamma}$	shear rate, s^{-1}
η	viscosity of a dispersion, Pa s
$[\eta]$	constant in the Krieger–Dougherty equation, –
η_0	zero-shear viscosity, Pa s
η_∞	infinite shear viscosity, Pa s
η_r	relative viscosity, –
η_s	viscosity of continuous phase, Pa s
η^*	complex viscosity, G^*/ω, Pa s
ϕ	volume fraction of dispersed phase, –
ϕ_G	volume fraction at beginning of glassy state, –
ϕ_{max}	maximum volume fraction of dispersed phase, –
ω	oscillatory frequency, rad s^{-1}

Figure 1 – Apparent viscosity versus shear rate data for several sodium caseinate dispersions; lines are Cross model fits

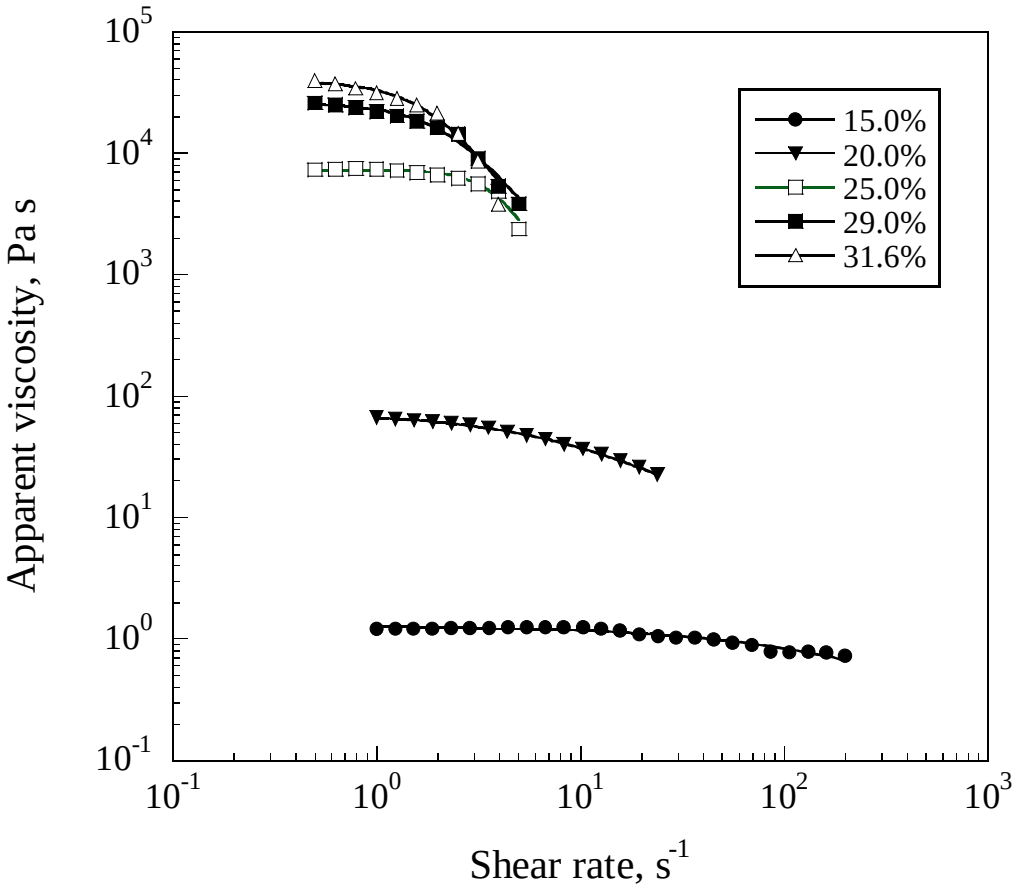

Figure 2 – Relative viscosity versus concentration. Data: open symbols, Farrer and Lips (1999); filled symbols, this work. Dashed line: estimated data of Panouille and others (2005). Solid line: Krieger–Dougherty model for hard spheres

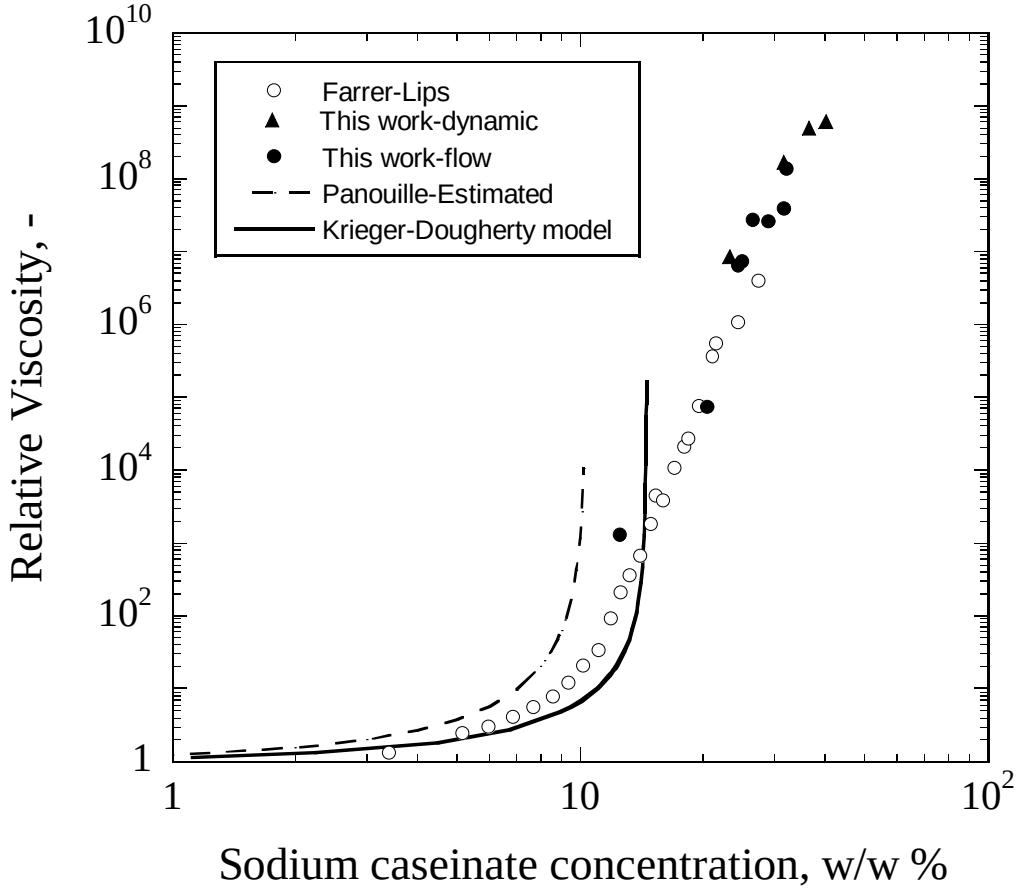

Figure 3 – *G'* (filled symbols) and *G"* (open symbols) versus frequency (ω) for sodium caseinate dispersions. At 20% w/w, values of *G'* were lower than those of *G"* at all values of ω; at 23% w/w, values of *G'* were greater than those of *G"* for $\omega > 2$ rad s^{-1}; at 31.6% w/w, *G'* > *G"* for $\omega > 0.3$ rad s^{-1}; at 40.1% w/w, *G'* > *G"* over the entire range of frequency

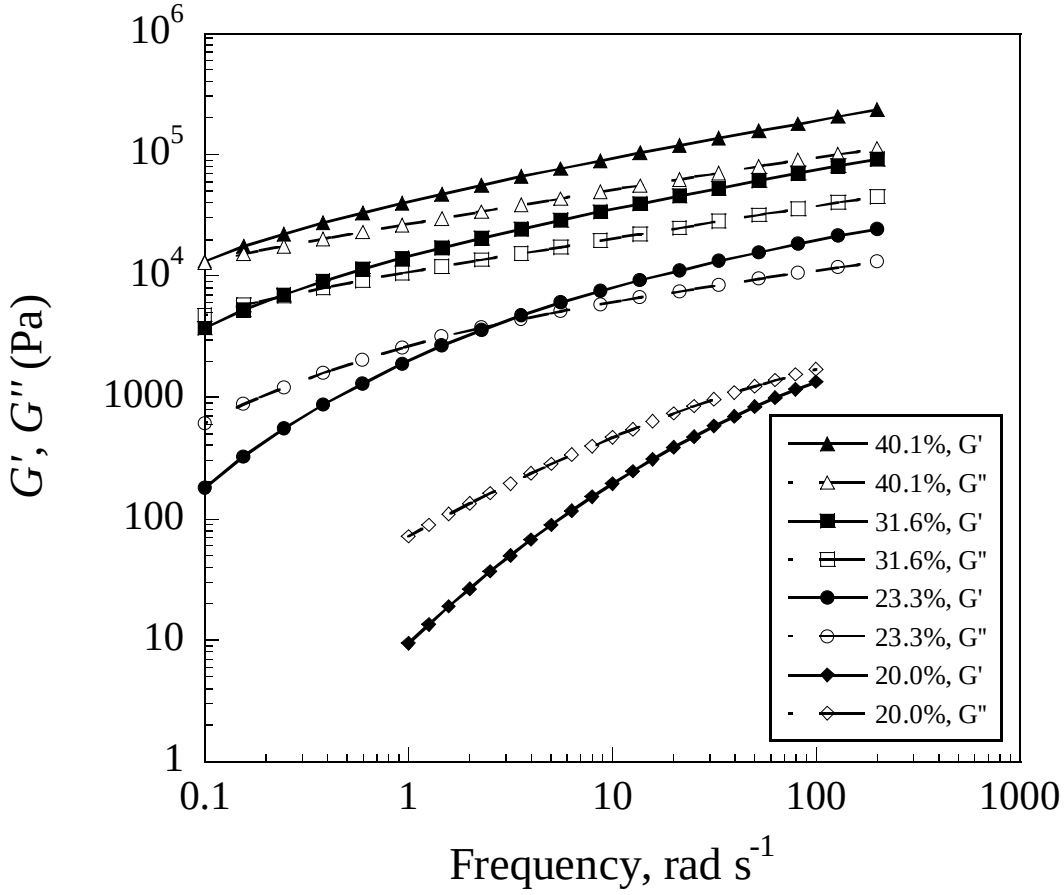

Figure 4 – Temperature sweep data for a 33.8% w/w sodium caseinate dispersion; the gelation (A) and softening (B) points are shown; for clarity, only every fifth point is shown

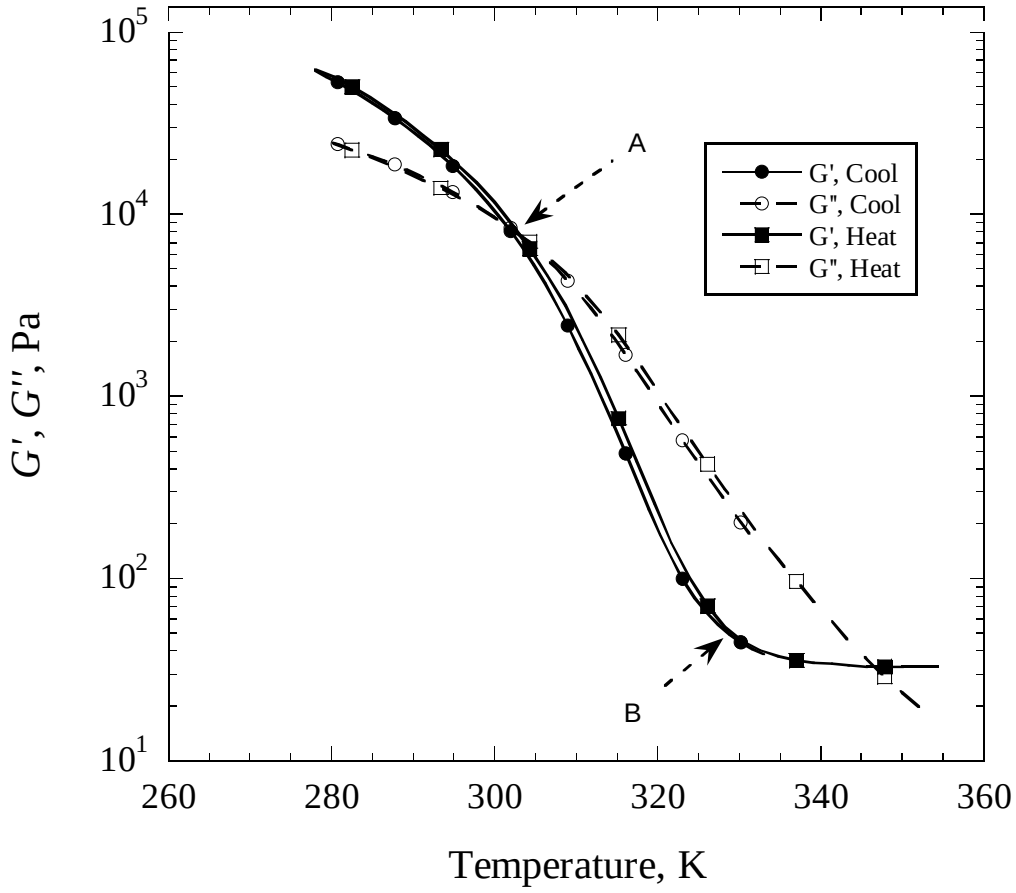

Figure 5 – Gelation and softening temperatures of sodium caseinate dispersions

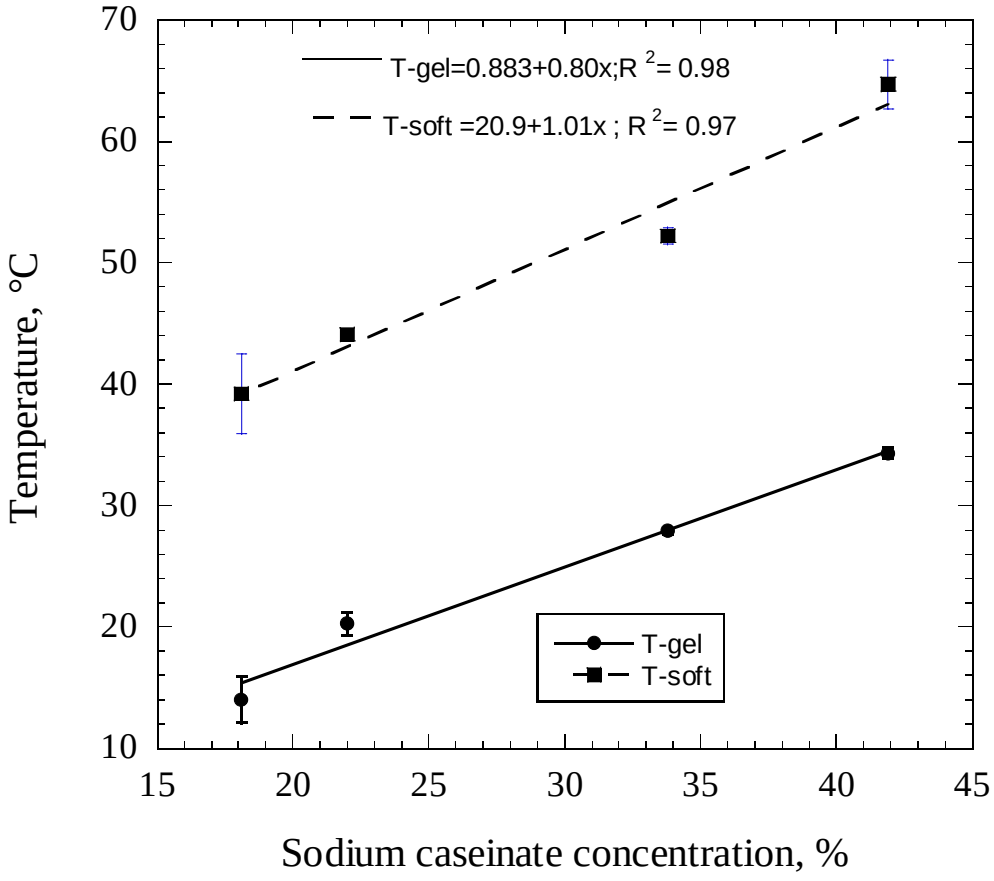

Figure 6 – Arrhenius plot to examine applicability of the Arrhenius model to the complex viscosity data of 18.1% and 41.9 % sodium caseinate dispersions. The filled symbols indicate the range of data over which the Arrhenius model was applicable.

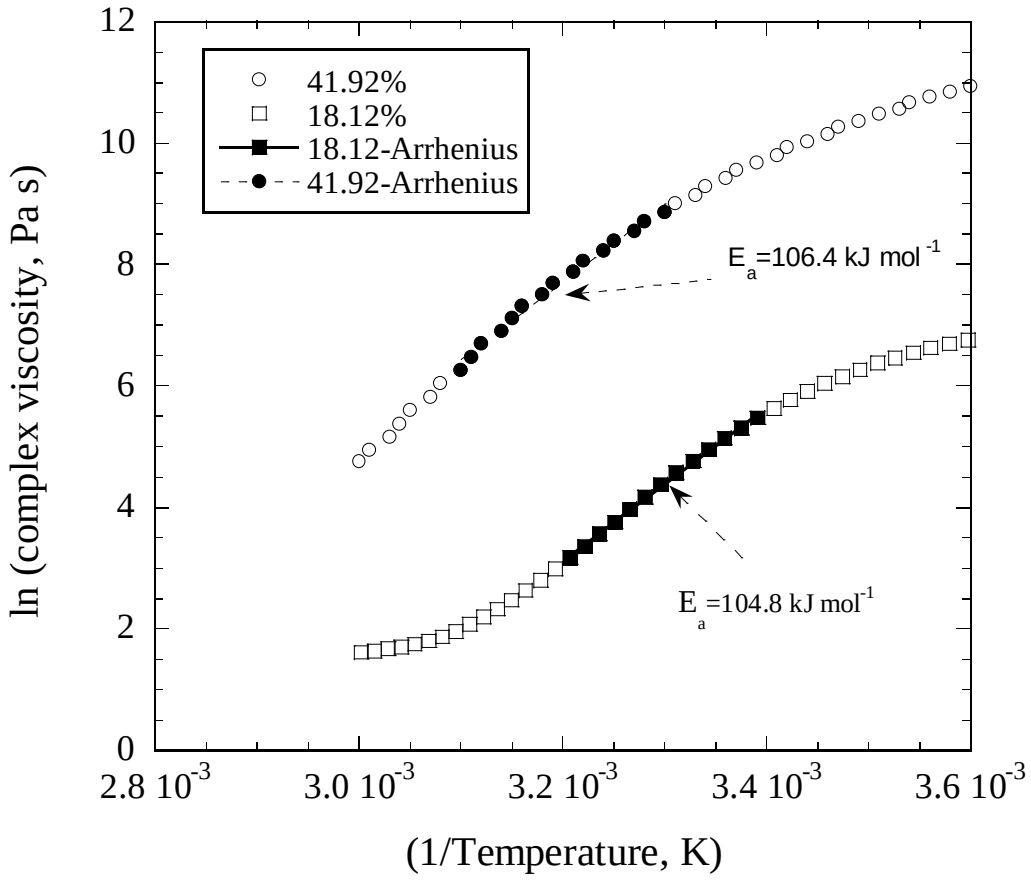

Figure 7 – Eldridge–Ferry plot to determine the enthalpy of softening of sodium caseinate dispersions.